ELSEVIER

Journal of Computational and Applied Mathematics 50 (1994) 67–83

JOURNAL OF
COMPUTATIONAL AND
APPLIED MATHEMATICS

A posteriori error estimation and adaptive mesh-refinement techniques

R. Verfürth

Fakultät für Mathematik, Ruhr-Universität Bochum, D-44780 Bochum Germany

Received 7 July 1992

Abstract

We analyse three different a posteriori error estimators for elliptic partial differential equations. They are based on the evaluation of local residuals with respect to the strong form of the differential equation, on the solution of local problems with Neumann boundary conditions, and on the solution of local problems with Dirichlet boundary conditions. We prove that all three are equivalent and yield global upper and local lower bounds for the true error. Thus adaptive mesh-refinement techniques based on these estimators are capable to detect local singularities of the solution and to appropriately refine the grid near these singularities. Some numerical examples prove the efficiency of the error estimators and the mesh-refinement techniques.

Key words: A posteriori error estimators; Adaptive mesh-refinement techniques; Elliptic partial differential equations

1. Introduction

In the numerical solution of practical problems of physics or engineering such as, e.g., computational fluid dynamics, elasticity, or semiconductor device simulation, one often encounters the difficulty that the overall accuracy of the numerical approximation is deteriorated by local singularities such as, e.g., singularities arising from re-entrant corners, interior or boundary layers, or sharp shock-like fronts. An obvious remedy is to refine the discretization near the critical regions, i.e., to place more grid-points where the solution is less regular. The question then is how to identify those regions and how to obtain a good balance between the refined and unrefined regions such that the overall accuracy is optimal.

Another closely related problem is to obtain reliable estimates of the accuracy of the computed numerical solution. A priori error estimates, as provided, e.g., by the standard error analysis for finite-element or finite-difference methods, are often insufficient, since they only yield information on the asymptotic error behaviour and require regularity assumptions about the solution which are not satisfied in the presence of singularities as described above.

SSDI 0377-0427(93)E0139-D

These considerations clearly show the need for an error estimator which can a posteriori be extracted from the computed numerical solution and the given data of the problem. Of course, the calculation of the a posteriori error estimate should be far less expensive than the computation of the numerical solution. Moreover, the error estimator should be local and should yield reliable upper and lower bounds for the true error in a user-specified norm. In this context one should note that global upper bounds are sufficient to obtain a numerical solution with an accuracy below a prescribed tolerance. Local lower bounds, however, are necessary to ensure that the grid is correctly refined so that one obtains a numerical solution with a prescribed tolerance using a (nearly) minimal number of grid-points. To achieve this task, it is not sufficient that the a posteriori error estimator has the same asymptotic behaviour as standard a priori error estimates.

In what follows we will present three a posteriori error estimators which are based on the evaluation of suitable local residuals (cf. [6,22,23,25]), the solution of suitable local Neumann-type problems (cf. [7–9,25]), and the solution of suitable local Dirichlet-type problems (cf. [5]), respectively. We will prove that — up to higher-order terms and constants, which are independent of the mesh-size — all of them yield global upper and local lower bounds for the true error and that these estimators are all equivalent. The proof of the upper bounds essentially relies on the consistency and stability of the discretization and on an integration by parts formula. The core of the proof of the lower bounds is a judicious choice of local test-functions. The equivalence of the error estimators and some of the lower bounds are new. In contrast to the results in [5–9], our proof does not require a super-approximation assumption of higher-order finite elements with respect to lower-order ones and does not depend on the polynomial degree of the underlying finite-element discretization. On the other hand, our estimators slightly differ from those given in [5–9]. They contain local projections of the data, and the size of the local problems that must be solved is slightly larger when using a linear finite-element discretization. The use of local projections of the data in combination with exact integration, however, is often equivalent to the use of the exact data in combination with a numerical quadrature rule.

In order to keep the formalism at a minimum and to make the ideas more transparent, we will restrict our analysis to a simple model problem: a conforming finite-element method for the two-dimensional Poisson equation with mixed Dirichlet–Neumann boundary conditions. The error estimators and the corresponding results, however, can be generalized to other discretizations such as, e.g., nonconforming finite-element or Petrov–Galerkin methods, and to more complicated problems such as, e.g., the two- or three-dimensional Navier–Stokes or elasticity equations or the equations used in semiconductor device simulation (cf. [22–25]). We will shortly comment on some of these generalizations.

Disposing of an a posteriori error estimator, an adaptive mesh-refinement process has the following general structure.

(1) Construct an initial coarse mesh $\mathcal{T}_0$ representing sufficiently well the geometry of the problem. Put $k := 0$.

(2) Solve the discrete problem on $\mathcal{T}_k$.

(3) For each element T in $\mathcal{T}_k$, compute the a posteriori error estimate.

(4) If the estimated global error is sufficiently small, then **stop**. Otherwise, decide which elements have to be refined and construct the next mesh $\mathcal{T}_{k+1}$. Replace k by $k+1$ and return to step (2).

This algorithm is best suited for stationary problems. For transient calculations it must be modified suitably (cf. [1–3,11,12,15,21]).

In what follows, we will describe some strategies to perform step (4) above, i.e., to choose the elements for refinement and to construct the next mesh. A more detailed overview on this topic may be found in [25] and the literature cited there. Numerical examples will show the efficiency of these strategies and of the a posteriori error estimators presented before.

2. The model problem and its discretization

We consider the Poisson equation with mixed Dirichlet–Neumann boundary conditions

$$-\Delta u = f, \quad \text{in } \Omega, \qquad u = g_{\mathrm{D}}, \quad \text{on } \Gamma_{\mathrm{D}}, \qquad \frac{\partial u}{\partial n} = g_{\mathrm{N}}, \quad \text{on } \Gamma_{\mathrm{N}}, \tag{2.1}$$

in a connected, bounded, polygonal domain $\Omega \subset \mathbb{R}^2$ with boundary Γ and $\Gamma_{\mathrm{D}} \cup \Gamma_{\mathrm{N}} = \Gamma$, $\Gamma_{\mathrm{D}} \cap \Gamma_{\mathrm{N}} = \emptyset$, $\Gamma_{\mathrm{D}} \neq \emptyset$.

For any open subset ω of Ω with Lipschitz boundary γ we denote by $L^2(\omega)$, $H^k(\omega)$ and $L^2(\gamma)$, $k \geqslant 1$, the standard Lebesgue and Sobolev spaces, respectively, equipped with the norms $\|\cdot\|_{0,\omega} := \|\cdot\|_{L^2(\omega)}$, $\|\cdot\|_{k,\omega} := \|\cdot\|_{H^k(\omega)}$ and $\|\cdot\|_{0,\gamma} := \|\cdot\|_{L^2(\gamma)}$. The inner products of $L^2(\omega)$ and $L^2(\gamma)$ are denoted by $(\cdot, \cdot)_\omega$ and $(\cdot, \cdot)_\gamma$, respectively.

Put

$$V := \{u \in H^1(\Omega) \colon u = 0 \text{ on } \Gamma_{\mathrm{D}}\}. \tag{2.2}$$

The standard weak formulation of problem (2.1) then is: Find $u \in g_{\mathrm{D}} + V$ such that

$$(\nabla u, \nabla v)_\Omega = (f, v)_\Omega + (g_{\mathrm{N}}, v)_{\Gamma_{\mathrm{N}}}, \quad \forall v \in V. \tag{2.3}$$

It is well known that problem (2.3) admits a unique solution.

Denote by $\mathcal{T}_h$ a family of triangulations of Ω which satisfies the following conditions.

(1) Any two triangles in $\mathcal{T}_h$ share at most a common edge or a common vertex.

(2) The triangulations are shape regular, i.e., for all triangles the ratio of the radius of the smallest circumscribed ball to that of the largest inscribed ball is bounded by a constant which does not depend on the triangle and on h.

Condition (2) is equivalent to the condition that the minimal angle of all triangles is bounded away from zero.

Denote by $P_{m,d}$, $m \geqslant 1$, $d \geqslant 1$, the space of polynomials of degree $\leqslant m$ in d variables and put

$$V_h := \{u \in C(\overline{\Omega}) \colon u|_T \in P_{k,2}, \forall T \in \mathcal{T}_h, u = 0 \text{ on } \Gamma_{\mathrm{D}}\}. \tag{2.4}$$

We then consider the following finite-element discretization of problem (2.3): Find $u_h \in g_{\mathrm{D}} + V_h$ such that

$$(\nabla u_h, \nabla v_h)_\Omega = (f, v_h)_\Omega + (g_{\mathrm{N}}, v_h)_{\Gamma_{\mathrm{N}}}, \quad \forall v_h \in V_h. \tag{2.5}$$

One easily checks that problem (2.5) admits a unique solution. For practical computations one usually will replace g_{D} by some suitable finite-element approximation $g_{\mathrm{D},h}$. This will introduce additional higher-order terms of the form $\|g_{\mathrm{D}} - g_{\mathrm{D},h}\|_{0,\Gamma_{\mathrm{D}}}$ in the estimates of Propositions 4.2–4.4 below.

In what follows, u and u_h will always refer to the unique solutions of problems (2.3) and (2.5), respectively. Moreover, c, c_1, $c_2,\dots$ will denote various constants which only depend on Ω and on the constant in condition (2) above.

3. The a posteriori error estimators

Before presenting the a posteriori error estimators, we introduce some notations.

For $T \in \mathcal{T}_h$ we denote by $\mathcal{E}(T)$ and $\mathcal{N}(T)$ the set of its edges and vertices, respectively. Let

$$\mathcal{E}_h := \bigcup_{T\in\mathcal{T}_h} \mathcal{E}(T), \qquad \mathcal{N}_h := \bigcup_{T\in\mathcal{T}_h} \mathcal{N}(T)$$

be the sets of all edges and vertices, respectively, in the triangulation. We split $\mathcal{E}_h$ and $\mathcal{N}_h$ in the form

$$\mathcal{E}_h = \mathcal{E}_{h,\Omega} \cup \mathcal{E}_{h,\mathrm{D}} \cup \mathcal{E}_{h,\mathrm{N}}, \qquad \mathcal{N}_h = \mathcal{N}_{h,\Omega} \cup \mathcal{N}_{h,\mathrm{D}} \cup \mathcal{N}_{h,\mathrm{N}},$$

with

$$\mathcal{E}_{h,\mathrm{D}} := \{E \in \mathcal{E}_h \colon E \subset \Gamma_{\mathrm{D}}\}, \quad \mathcal{E}_{h,\mathrm{N}} := \{E \in \mathcal{E}_h \colon E \subset \Gamma_{\mathrm{N}}\},$$
$$\mathcal{N}_{h,\mathrm{D}} := \{x \in \mathcal{N}_h \colon x \in \Gamma_{\mathrm{D}}\}, \quad \mathcal{N}_{h,\mathrm{N}} := \{x \in \mathcal{N}_h \colon x \in \Gamma_{\mathrm{N}}\}.$$

For $T \in \mathcal{T}_h$ and $E \in \mathcal{E}_h$, we denote by h_T and h_E their diameter and length, respectively. Condition (2) Section 2 implies that all the ratios h_T/h_E, $T \in \mathcal{T}_h$, $E \in \mathcal{E}(T)$, and $h_T/h_{T'}$, T, $T' \in \mathcal{T}_h$, $\mathcal{N}(T) \cap \mathcal{N}(T') \neq 0$, are bounded from above and from below by constants which only depend on the constant in condition (2).

For $T \in \mathcal{T}_h$, $E \in \mathcal{E}_h$ and $x \in \mathcal{N}_h$ let

$$\omega_T := \bigcup_{\mathcal{E}(T)\cap\mathcal{E}(T')\neq 0} T', \qquad \omega_E := \bigcup_{E\in\mathcal{E}(T')} T', \qquad \omega_x := \bigcup_{x\in\mathcal{N}(T')} T'$$

(see Fig. 1) and put

$$V_T := \{\phi \in C(T) \colon \phi \in \Pi_{\max\{k+1,3\},2},\ \phi|_E \in \Pi_{k+1,1},\ \forall E \in \mathcal{E}(T),$$
$$\phi(x) = 0,\ \forall x \in \mathcal{N}(T),\ \phi|_E = 0,\ \forall E \in \mathcal{E}(T) \cap \mathcal{E}_{h,\mathrm{D}}\}, \tag{3.1}$$

$$V_x := \{\phi \in C(\bar{\omega}_x) \colon \phi|_{T'} \in V_{T'},\ \forall T' \subset \omega_x,\ \phi = 0 \text{ on } \partial\omega_x \backslash \Gamma_{\mathrm{N}}\}. \tag{3.2}$$

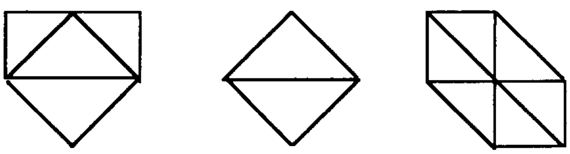

Fig. 1. Domains ω_T, ω_E and ω_x.

Moreover, denote by ψ_T and ψ_E cut-off functions which are uniquely defined by the following properties:

$$\operatorname{supp} \psi_T \subset T, \qquad \psi_T \in \Pi_{3,2}, \qquad \psi_T \geqslant 0, \qquad \max_{x \in T} \psi_T(x) = 1, \tag{3.3}$$

and

$$\operatorname{supp} \psi_E \subset \omega_E, \qquad \psi_{E|T'} \in \Pi_{2,2}, \ \forall T' \subset \omega_E, \qquad \psi_E \geqslant 0, \qquad \max_{x \in \omega_E} \psi_E(x) = 1. \tag{3.4}$$

Given $E \in \mathscr{E}_{h,\Omega}$ and $\phi \in L^2(\omega_E)$ with $\phi|_{T'} \in C(T')$, $\forall T' \subset \omega_E$, we denote by $[\phi]_E$ the jump of ϕ across E in an arbitrary, but fixed direction. Put

$$R_E(u_h) := \begin{cases} -\left[\dfrac{\partial u_h}{\partial n}\right]_E, & \forall E \in \mathscr{E}_{h,\Omega}, \\ \Pi_E g_{\mathrm{N}} - \dfrac{\partial u_h}{\partial n}, & \forall E \in \mathscr{E}_{h,\mathrm{N}}, \\ 0, & \forall E \in \mathscr{E}_{h,\mathrm{D}}, \end{cases} \tag{3.5}$$

and

$$R_T(u_h) := \Pi_T f + \Delta u_h, \quad \forall T \in \mathscr{T}_h, \tag{3.6}$$

where Π_E and Π_T are the L^2 projectors of $L^2(\Gamma_N)$ and $L^2(\Omega)$ onto the space of piecewise constant functions with respect to $\mathscr{E}_{h,N}$ and $\mathscr{T}_h$.

The first error estimator simply is a weighted combination of the residuals $R_T(u_h)$ and $R_E(u_h)$. It is given by

$$\eta_{T,R} := \left\{ h_T^2 \| R_T(u_h) \|_{0,T}^2 + \sum_{E \in \mathscr{E}(T) \setminus \mathscr{E}_{h,\mathrm{D}}} h_E \| R_E(u_h) \|_{0,E}^2 \right\}^{1/2}, \quad \forall T \in \mathscr{T}_h. \tag{3.7}$$

This estimator was first proposed and analysed for problem (2.1) in one dimension in [6]. It was generalized to the Navier–Stokes equations in [22–25].

The second error estimator is based on the solution of local Neumann problems. For any $T \in \mathscr{T}_h$, it is given by

$$\eta_{T,\mathrm{N}} := \| \nabla u_{T,\mathrm{N}} \|_{0,T}, \tag{3.8}$$

where $u_{T,\mathrm{N}} \in V_T$ is the unique solution of

$$(\nabla u_{T,\mathrm{N}}, \nabla v_T)_T = (R_T(u_h), v_T)_T + \sum_{E \in \mathscr{E}(T) \setminus \mathscr{E}_{h,\mathrm{D}}} (R_E(u_h), v_T)_E, \quad \forall v_T \in V_T. \tag{3.9}$$

Problem (3.9) is a discrete version of the following Poisson equation with mixed Neumann–Dirichlet boundary conditions:

$$\begin{aligned} -\Delta \phi &= R_T(u_h), && \text{in } T, \\ \psi &= 0, && \text{on } \partial T \cap \Gamma_{\mathrm{D}}, \\ \frac{\partial \phi}{\partial n} &= R_E(u_h), && \text{on } \partial T \setminus \Gamma_{\mathrm{D}}. \end{aligned}$$

It admits a unique solution since the functions in V_T vanish at the vertices of T. The estimator $\eta_{T,\mathrm{N}}$ was first analysed in [7] and then generalized to the Navier–Stokes equations in [8,9,22–25].

The third error estimator is based on the solution of local Dirichlet problems. For any $x \in \mathcal{N}_{h,\Omega} \cup \mathcal{N}_{h,\mathrm{N}}$, it is given by

$$\eta_{x,\mathrm{D}} := \|\nabla(u_{x,\mathrm{D}} - u_h)\|_{0,\omega_x}, \tag{3.10}$$

where $u_{x,\mathrm{D}} \in u_h + V_x$ is the unique solution of

$$(\nabla u_{x,\mathrm{D}}, \nabla v_x)_{\omega_x} = (\Pi_T f, v_x)_{w_x} + (\Pi_E g_\mathrm{N}, v_x)_{\partial\omega_x \cap \Gamma_\mathrm{N}}, \quad \forall v_x \in V_x. \tag{3.11}$$

Problem (3.11) is a discrete version of the following Poisson equation with mixed Neumann–Dirichlet boundary conditions:

$$\begin{aligned} -\Delta\psi &= \Pi_T f, && \text{in } \omega_x, \\ \psi &= u_h, && \text{on } \partial\omega_x \setminus \Gamma_\mathrm{N}, \\ \frac{\partial\psi}{\partial n} &= \Pi_E g_\mathrm{N}, && \text{on } \partial\omega_x \cap \Gamma_\mathrm{N}. \end{aligned}$$

The estimator $\eta_{x,\mathrm{D}}$ was introduced in [5].

Obviously, the evaluation of $\eta_{T,R}$ requires less work than the evaluation of $\eta_{T,\mathrm{N}}$, which in its turn is less expensive than the evaluation of $\eta_{x,\mathrm{D}}$.

We end this section with some general remarks on the principal structure of the error estimators described above and their generalization to more complicated problems.

(1) For low-order finite-element methods, the jump terms $R_E(u_h)$ are crucial. Consider, for example, the case of a harmonic function, i.e., problem (2.1) with $f = 0$ and $\Gamma_\mathrm{D} = \Gamma$, and its approximation by continuous, piecewise linear functions, i.e., $k = 1$. Then $R_T(u_h) = 0, \forall T \in \mathcal{T}_h$, $u_h \in V_h$, but u_h is of course not harmonic, since it is not contained in $H^2(\Omega)$. The jumps of the normal derivatives, i.e., $R_E(u_h)$, measure the discrepancy between $H^1(\Omega)$ and $H^2(\Omega)$. Equation (4.22) below shows that the $R_E(u_h)$-terms are also implicitly present in $\eta_{x,\mathrm{D}}$.

(2) $R_T(u_h)$ is the residual on T of u_h with respect to the strong form of the differential equation. $R_E(u_h)$ is the jump across E of that boundary operator applied to u_h that is canonically associated with the strong and the weak form of the differential equation. Thus, $R_E(u_h)$ is only effected by the principal part of the differential operator. If one adds, e.g., a convection term $b\,\nabla u$ to equation (2.1), $R_E(u_h)$ remains unchanged whereas a term $b\,\nabla u_h$ must be added to $R_T(u_h)$.

(3) Problems (3.9) and (3.11) are local analogues of problem (2.5) using higher-order elements. For nonlinear problems, however, one can linearize the local problems around the computed numerical solution u_h. For the Navier–Stokes equations, e.g., it is thus sufficient to solve local Stokes problems. In the local problems one can similarly neglect lower-order terms of the differential operator, provided the local mesh-size is small enough. Thus, one can, e.g., neglect the convection $b\,\nabla u$ if the local Peclet number $h_T\|b\|_{L^\infty(T)}$ is small enough.

(4) For the model problem it is quite easy to check that problems (3.9) and (3.11) are well-posed. For other problems such as, e.g., the Stokes equations one has to carefully choose the finite-element spaces V_T and V_x in order to obtain well-posed local problems (cf. [22,25]).

(5) The proof of the lower bounds of Propositions 4.2–4.4 below relies on the fact that $R_T(u_h)$ and $R_E(u_h)$ belong to finite-dimensional spaces. Thus it requires the approximation of f and g_N by suitable piecewise polynomial functions. It is, however, not necessary to use piecewise constant approximations or L^2 projections. We restrict ourselves to this choice simply for convenience. The approximation of the data f and g_N is not used in [5–7]. For practical computations, however, the terms appearing on the right-hand side of (3.7), (3.9) and (3.11) must be evaluated by some numerical quadrature rule. In many cases this is equivalent to the use of a finite-element approximation of the data in combination with exact integration.

4. Lower and upper bounds for the error estimators

We first construct an extension operator $P: C(E) \to C(T)$, $T \in \mathscr{T}_h$, $E \in \mathscr{E}(T)$, which maps $P_{m,1}$, $m \in \mathbb{N}$, into $P_{m,2}$. To this end, let $\hat{T}$ be the reference triangle with vertices (0, 0), (1, 0) and (0, 1), and $\hat{E}$ the edge $[0, 1] \times \{0\}$ of $\hat{T}$. Denote by $F_T: \mathbb{R}^2 \to \mathbb{R}^2$ the orientation-preserving affine transformation which maps $\hat{T}$ onto T and $\hat{E}$ onto E. Define the extension operator $\hat{P}: C(\hat{E}) \to C(\hat{T})$ by

$$\hat{P}\hat{\sigma}(x, y) = \hat{\sigma}(x), \quad \forall \hat{\sigma} \in C(\hat{E}), \qquad (x, y) \in \hat{T}. \tag{4.1}$$

Then P is given by

$$P\sigma := \left[\hat{P}(\sigma \circ F_T)\right] \circ F_T^{-1}, \quad \forall \sigma \in C(E). \tag{4.2}$$

Note that $P\sigma$ is constant along lines parallel to E' where E' is the edge of T which has the left end-point of E as its right end-point. Here, the orientation of edges is induced by the exterior normal of T (see Fig. 2).

Lemma 4.1. *Let $m \in \mathbb{N}$. There exist constants $c_1, \ldots, c_4$, which only depend on m and the constant in condition* (2) *of Section* 2, *such that the following inequalities hold for all $T \in \mathscr{T}_h$, $E \in \mathscr{E}(T)$, $\phi \in L^2(T) \cap P_{m,2}$, $\sigma \in L^2(E) \cap P_{m,1}$:*

$$\|\psi_T \phi\|_{0,T} \leqslant \|\phi\|_{0,T}, \tag{4.3}$$

$$\|\psi_T^{1/2} \phi\|_{0,T} \geqslant c_1 \|\phi\|_{0,T}, \tag{4.4}$$

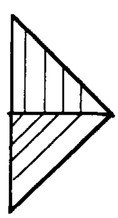

Fig. 2. Level lines of $P\sigma$.

$$\|\psi_E\sigma\|_{0,E} \leqslant \|\sigma\|_{0,E}, \tag{4.5}$$

$$\|\psi_E^{1/2}\sigma\|_{0,E} \geqslant c_2\|\sigma\|_{0,E}, \tag{4.6}$$

$$c_3 h_E^{1/2}\|\sigma\|_{0,E} \leqslant \|\psi_E^{1/2}P\sigma\|_{0,T} \leqslant c_4 h_E^{1/2}\|\sigma\|_{0,E}. \tag{4.7}$$

Proof. Inequalities (4.3) and (4.5) immediately follow from $0 \leqslant \psi_T \leqslant 1$, $0 \leqslant \psi_E \leqslant 1$.

In order to prove the inequalities (4.4) and (4.6), we define $\hat{\phi} := \phi \circ F_T$ and $\hat{\sigma} := \sigma \circ F_T$. Observing that $\psi_T \circ F_T = \psi_{\hat{T}}$ and $\psi_E \circ F_T = \psi_{\hat{E}}$, we obtain

$$\|\psi_T^{1/2}\phi\|_{0,T} = |\det DF_T|^{1/2}\|\psi_{\hat{T}}^{1/2}\hat{\phi}\|_{0,\hat{T}}, \quad \|\phi\|_{0,T} = |\det DF_T|^{1/2}\|\hat{\phi}\|_{0,\hat{T}},$$

$$\|\psi_E^{1/2}\sigma\|_{0,E} = h_E^{1/2}\|\psi_{\hat{E}}^{1/2}\hat{\sigma}\|_{0,\hat{E}}, \quad \|\sigma\|_{0,E} = h_E^{1/2}\|\hat{\sigma}\|_{0,\hat{E}}.$$

The inequalities now follow from the fact that all norms are equivalent on the finite-dimensional spaces $P_{m,2}$ and $P_{m,1}$, respectively.

Inequality (4.7) finally follows from the above equations, the identity

$$\|\psi_E^{1/2}P\sigma\|_{0,T} = |\det DF_T|^{1/2}\|\psi_{\hat{E}}^{1/2}\hat{P}\hat{\sigma}\|_{0,\hat{T}},$$

the estimate

$$\underline{c}h_E \leqslant |\det DF_T|^{1/2} \leqslant \bar{c}h_E,$$

where $\underline{c}$, $\bar{c}$ only depend on the constant in condition (2) of Section 2, and the fact that $\|\psi_{\hat{E}}^{1/2}\hat{P}\hat{\sigma}\|_{0,\hat{T}}$ defines a norm on $P_{m,1}$ which is equivalent to $\|\hat{\sigma}\|_{0,\hat{E}}$. □

Now we are ready to prove that the error estimator $\eta_{T,R}$ yields global upper and local lower bounds for the error $\|u-u_h\|_{1,\Omega}$.

Proposition 4.2. *There are constants c_5, c_6, which only depend on the polynomial degree k and the constant in condition (2) of Section 2, such that*

$$\|u-u_h\|_{1,\Omega} \leqslant c_5\left\{\sum_{T\in\mathcal{T}_h}\eta_{T,R}^2 + \sum_{T\in\mathcal{T}_h}h_T^2\|f-\Pi_T f\|_{0,T}^2 + \sum_{E\in\mathcal{E}_{h,\mathrm{N}}}h_E\|g_\mathrm{N}-\Pi_E g_\mathrm{N}\|_{0,E}^2\right\}^{1/2} \tag{4.8}$$

and

$$\eta_{T,R} \leqslant c_6\left\{\|u-u_h\|_{1,\omega_T}^2 + \sum_{T'\subset\omega_T}h_{T'}^2\|f-\Pi_T f\|_{0,T'}^2 + \sum_{E\in\mathcal{E}(T)\cap\mathcal{E}_{h,\mathrm{N}}}h_E\|g_\mathrm{N}-\Pi_E g_\mathrm{N}\|_{0,E}^2\right\}^{1/2}, \quad \forall T\in\mathcal{T}_h. \tag{4.9}$$

Proof. Denote by I_h the operator which associates with each $w\in H^2(\Omega)$ the continuous piecewise linear function interpolating w in the points of $\mathcal{N}_h$. Let $w\in H^2(\Omega)$ with $w=0$ on Γ_D be arbitrary. We then have $I_h w\in V_h\subset V$ and

$$\|w-I_h w\|_{0,T} \leqslant c_7 h_T\|\nabla w\|_{0,T}, \quad \forall T\in\mathcal{T}_h,$$

$$\|w-I_h w\|_{0,E} \leqslant c_8 h_E^{1/2}\|\nabla w\|_{0,\omega_E}, \quad \forall E\in\mathcal{E}_h.$$

Using the orthogonality

$$(\nabla(u-u_h), \nabla v_h)_\Omega = 0, \quad \forall v_h \in V_h, \tag{4.10}$$

and integration by parts, we obtain

$$\begin{aligned}
(\nabla(u-u_h), \nabla w)_\Omega &= (\nabla(u-u_h), \nabla(w-I_h w))_\Omega \\
&= (f, w-I_h w)_\Omega + (g_N, w-I_h w)_{\Gamma_N} \\
&\quad + \sum_{T\in\mathcal{T}_h} \left\{ (\Delta u_h, w-I_h w)_T - \left(\frac{\partial u_h}{\partial n}, w-I_h w\right)_{\partial T} \right\} \\
&= \sum_{T\in\mathcal{T}_h} (R_T(u_h) + f - \Pi_T f, w-I_h w)_T + \sum_{E\in\mathcal{E}_{h,\Omega}} (R_E(u_h), w-I_h w)_E \\
&\quad + \sum_{E\in\mathcal{E}_{h,N}} (R_E(u_h) + g_N - \Pi_E g_N, w-I_h w)_E \\
&\leqslant c_7 \sum_{T\in\mathcal{T}_h} \{h_T \|R_T(u_h)\|_{0,T} + h_T\|f-\Pi_T f\|_{0,T}\} \|\nabla w\|_{0,T} \\
&\quad + c_8 \sum_{E\in\mathcal{E}_{h,\Omega}} h_E^{1/2} \|R_E(u_h)\|_{0,E} \|\nabla w\|_{0,\omega_E} \\
&\quad + c_8 \sum_{E\in\epsilon_{h,N}} \{h_E^{1/2}\|R_E(u_h)\|_{0,E} + h_E^{1/2}\|g_N - \Pi_E g_N\|_{0,E}\} \|\nabla w\|_{0,\omega_E} \\
&\leqslant c_9 \|w\|_{1,\Omega} \left\{ \sum_{T\in\mathcal{T}_h} \eta_{T,R}^2 + \sum_{T\in\mathcal{T}_h} h_T^2 \|f-\Pi_T f\|_{0,T}^2 \right. \\
&\quad \left. + \sum_{E\in\mathcal{E}_{h,N}} h_E \|g_N - \Pi_E g_N\|_{0,E}^2 \right\}^{1/2}.
\end{aligned}$$

This proves inequality (4.8) since $\{w\in H^2(\Omega)\colon w=0 \text{ on } \Gamma_D\}$ is dense in V and since

$$\sup_{\substack{v\in V \\ \|v\|_{1,\Omega}=1}} (\nabla(u-u_h), \nabla v) \geqslant c_0 \|u-u_h\|_{1,\Omega}. \tag{4.11}$$

In order to prove inequality (4.9), let $T\in\mathcal{T}_h$. Let $w\in H^1(\omega_T)$ with $w=0$ on $\partial\omega_T \setminus (\partial T\cap\Gamma_N)$. Extending w by 0 outside ω_T to a function in V and using integration by parts for the u_h-terms, we obtain

$$\begin{aligned}
\epsilon(w) &:= \sum_{T'\subset\omega_T} (R_{T'}(u_h), w)_{T'} + \sum_{E\in\mathcal{E}(T)\setminus\mathcal{E}_{h,D}} (R_E(u_h), w)_E \\
&= (\Pi_T f - f, w)_{\omega_T} + (\nabla(u-u_h), \nabla w)_{\omega_T} + (\Pi_E g_N - g_N, w)_{\partial T\cap\Gamma_N}.
\end{aligned} \tag{4.12}$$

Let $T'\subset\omega_T$ and put $w_{T'} := \psi_{T'} R_{T'}(u_h)$. Observing that supp $w_{T'}\subset T'$ and

$$\|\nabla w_{T'}\|_{0,T'} \leqslant c_{10} h_{T'}^{-1} \|w_{T'}\|_{0,T'},$$

we conclude from Lemma 4.1 and (4.12) that

$$c_1^2\|R_{T'}(u_h)\|_{0,T'}^2 \leqslant \epsilon(w_{T'})$$
$$\leqslant \|R_{T'}(u_h)\|_{0,T'}\left\{\|f-\Pi_T f\|_{0,T'} + c_{10}h_{T'}^{-1}\|\nabla(u-u_h)\|_{0,T'}\right\},$$

and thus

$$\|R_{T'}(u_h)\|_{0,T'} \leqslant c_{11}\|f-\Pi_T f\|_{0,T'} + c_{12}h_{T'}^{-1}\|\nabla(u-u_h)\|_{0,T'}. \tag{4.13}$$

Let $E\in\mathscr{E}(T)\cap\mathscr{E}_{h,\Omega}$ and put $w_E := \psi_E P(R_E(u_h))$. Using

$$\|\nabla w_E\|_{0,\omega_E} \leqslant c_{13}h_E^{-1}\|w_E\|_{0,\omega_E},$$

we obtain from Lemma 4.1 and (4.12) and (4.13) that

$$\begin{aligned} c_2^2\|R_E(u_h)\|_{0,E}^2 &\leqslant \epsilon(w_E) - \sum_{T''\subset\omega_E}(R_{T''}(u_h), w_E)_{T''} \\ &\leqslant \|R_E(u_h)\|_{0,E} \\ &\quad\times \sum_{T''\subset\omega_E}\left\{c_4h_E^{1/2}\|f-\Pi_T f\|_{0,T''} + c_4c_{13}h_E^{-1/2}\|\nabla(u-u_h)\|_{0,T''} + c_4h_E^{1/2}\|R_{T''}(u_h)\|_{0,T''}\right\} \\ &\leqslant \|R_E(u_h)\|_{0,E}\sum_{T''\subset\omega_E}\left\{c_{14}h_E^{1/2}\|f-\Pi_T f\|_{0,T''} + c_{15}h_E^{-1/2}\|\nabla(u-u_h)\|_{0,T''}\right\}, \end{aligned}$$

and thus

$$\|R_E(u_h)\|_{0,E} \leqslant \sum_{T''\subset\omega_E}\left\{c_{16}h_E^{1/2}\|f-\Pi_T f\|_{0,T''} + c_{17}h_E^{-1/2}\|\nabla(u-u_h)\|_{0,T''}\right\}. \tag{4.14}$$

Now, let $E\in\mathscr{E}(T)\cap\mathscr{E}_{h,\mathrm{N}}$ and $w_E := \psi_E P(R_E(u_h))$. Observing that in this case $\omega_E = T$, we obtain with the same arguments as above

$$\begin{aligned} c_2^2\|R_E(u_h)\|_{0,E}^2 &\leqslant \epsilon(w_E) - (R_T(u_h), w_E)_T \\ &\leqslant \|R_E(u_h)\|_{0,E}\left\{c_4h_E^{1/2}\|f-\Pi_T f\|_{0,T} + c_4c_{13}h_E^{-1/2}\|\nabla(u-u_h)\|_{0,T}\right. \\ &\qquad \left. + c_4h_E^{1/2}\|R_T(u_h)\|_{0,T} + \|g_\mathrm{N} - \Pi_E g_\mathrm{N}\|_{0,E}\right\}, \end{aligned}$$

and thus

$$\|R_E(u_h)\|_{0,E} \leqslant c_{17}h_E^{-1/2}\|\nabla(u-u_h)\|_{0,T} + c_{16}h_E^{1/2}\|f-\Pi_T f\|_{0,T} + c_2^{-2}\|g_\mathrm{N} - \Pi_E g_\mathrm{N}\|_{0,E}. \tag{4.15}$$

Estimates (4.13)–(4.15) immediately imply inequality (4.9). □

Before considering the other error estimators, we want to make some remarks concerning Proposition 4.2 and its proof.

(1) The terms $h_T\|f-\Pi_T f\|_{0,T}$ and $h_E^{1/2}\|g_\mathrm{N} - \Pi_E g_\mathrm{N}\|_{0,E}$ are higher-order perturbations.

(2) The stability estimate (4.11) is a consequence of the coercivity result

$$\|\nabla u\|_{0,\Omega}^2 \geqslant c_0\|u\|_{1,\Omega}^2, \quad \forall u\in V.$$

We prefer estimate (4.11) upon the above estimate, since an analogon of the former also holds for more complicated problems such as, e.g., the Stokes equations, whereas an analogon to the latter is no longer valid.

(3) The orthogonality (4.10) follows from the conformity of the finite-element spaces. For nonconforming methods, the consistency error then appears on the right-hand side of (4.10). Proposition 4.2 still holds, provided the consistency error is a higher-order perturbation as the terms discussed in (1) above. The same remark applies to certain Petrov–Galerkin methods where higher-order terms used for the stabilization of the method appear on the right-hand side of (4.10) (cf., e.g., [24,25]).

The following proposition shows that the error estimators $\eta_{T,R}$ and $\eta_{T,\mathrm{N}}$ are essentially equivalent. Combined with Proposition 4.2 it implies bounds for $\eta_{T,\mathrm{N}}$ similar to inequalities (4.8) and (4.9).

Proposition 4.3. *The following estimates hold for all $T \in \mathscr{T}_h$:*

$$\eta_{T,\mathrm{N}} \leqslant c_{18} \eta_{T,R}, \tag{4.16}$$

$$\eta_{T,R} \leqslant c_{19} \left\{ \sum_{T' \subset \omega_T} \eta_{T',\mathrm{N}}^2 \right\}^{1/2}, \tag{4.17}$$

where c_{18}, c_{19} only depend on the polynomial degree k and the constant in condition (2) *of Section* 2.

Proof. Consider an arbitrary $T \in \mathscr{T}_h$. Since the functions in V_T vanish at the nodes of T, we have

$$\|\phi\|_{0,T} \leqslant c_{20} h_T \|\nabla \phi\|_{0,T}, \quad \forall \phi \in V_T,\ T \in \mathscr{T}_h,$$

$$\|\phi\|_{0,E} \leqslant c_{21} h_E^{1/2} \|\nabla \phi\|_{0,T}, \quad \forall \phi \in V_T,\ T \in \mathscr{T}_h,\ E \in \mathscr{E}(T).$$

Taking $u_{T,\mathrm{N}}$ as test-function in (3.9) and using the above estimates, we immediately obtain inequality (4.16).

In order to prove inequality (4.17), let $T' \subset \omega_T$ and $E \in \mathscr{E}(T) \backslash \mathscr{E}_{h,\mathrm{D}}$. Observing that the functions $w_{T'}$ and w_E used in the proof of Proposition 4.2 are admissible test-functions for problem (3.9) corresponding to T' and T'' with $E \in \mathscr{E}(T'')$, we conclude that

$$c_1^2 \|R_{T'}(u_h)\|_{0,T'}^2 \leqslant \epsilon(w_{T'}) = (\nabla u_{T',\mathrm{N}}, \nabla w_{T'})_{T'} \leqslant c_{22} h_{T'}^{-1} \|R_{T'}(u_h)\|_{0,T'} \eta_{T',\mathrm{N}} \tag{4.18}$$

and

$$\begin{aligned} c_2^2 \|R_E(u_h)\|_{0,E}^2 &\leqslant (R_E(u_h), w_E)_E \\ &= \frac{1}{n_E} \sum_{T'' \subset \omega_E} \left\{ (\nabla u_{T'',\mathrm{N}}, \nabla w_E)_{T''} - (R_{T''}(u_h), w_E)_{T''} \right\} \\ &\leqslant c_{23} \|R_E(u_h)\|_{0,E} \sum_{T'' \subset \omega_E} \left\{ h_E^{-1/2} \eta_{T'',\mathrm{N}} + h_E^{1/2} \|R_{T''}(u_h)\|_{0,T''} \right\}, \end{aligned} \tag{4.19}$$

where $n_E \in \{1, 2\}$ is the number of triangles sharing the edge E. Estimates (4.18) and (4.19) immediately imply inequality (4.17). □

The next proposition shows that the error estimators $\eta_{x,\mathrm{D}}$ and $\eta_{T,R}$ and, hence, $\eta_{x,\mathrm{D}}$ and $\eta_{T,\mathrm{N}}$, too, are essentially equivalent. Together with Proposition 4.2 it implies bounds for $\eta_{x,\mathrm{D}}$ similar to inequalities (4.8) and (4.9).

Proposition 4.4. *The following estimates hold for all* $x \in \mathscr{N}_{h,\Omega} \cup \mathscr{N}_{h,\mathrm{N}}$:

$$\eta_{x,\mathrm{D}} \leqslant c_{24} \Big\{ \sum_{T' \subset \omega_x} \eta_{T',R}^2 \Big\}^{1/2}, \tag{4.20}$$

$$\eta_{T,R} \leqslant c_{25} \Big\{ \sum_{x' \in \mathscr{N}(T) \setminus \mathscr{N}_{h,\mathrm{D}}} \eta_{x',\mathrm{D}}^2 \Big\}^{1/2}, \tag{4.21}$$

where c_{24}, c_{25} *only depend on the polynomial degree k and the constant in condition* (2) *of Section* 2.

Proof. Consider an arbitrary $x \in \mathscr{N}_{h,\Omega} \cup \mathscr{N}_{h,\mathrm{N}}$. Integration by parts of the u_h-terms and (3.11) yield

$$\begin{aligned}(\nabla(u_{x,\mathrm{D}} - u_h), \nabla v_x)_{\omega_x} = \sum_{T' \subset \omega_x} \Big\{ (R_{T'}(u_h), v_x)_{T'} + \sum_{\substack{E' \in \mathscr{E}(T') \\ x \in E'}} (R_{E'}(u_h), v_x)_{E'} \Big\} \\ + \sum_{E \subset \partial\omega_x \cap \Gamma_\mathrm{N}} (R_E(u_h), v_x)_E, \quad \forall v_x \in V_x.\end{aligned} \tag{4.22}$$

Taking $u_{x,\mathrm{D}} - u_h$ as test-function and observing that $(u_{x,\mathrm{D}} - u_h)|_{T'} \in V_{T'}$, $\forall T' \subset \omega_x$, this implies inequality (4.20).

In order to prove the inequality (4.21), consider an arbitrary $T \in \mathscr{T}_h$. Let $T' \subset \omega_T$ and $E \in \mathscr{E}(T) \setminus \mathscr{E}_{h,\mathrm{D}}$. Observing that the functions $w_{T'}$ and w_E used in the proof of Proposition 4.2 are admissible test-functions for problem (3.11) corresponding to $x \in \mathscr{N}(T')$ and $x \in E$, respectively, we conclude from (4.22) that

$$\begin{aligned}c_1^2 \| R_{T'}(u_h) \|_{0,T'}^2 \leqslant \epsilon(w_{T'}) &= \frac{1}{n_x} \sum_{x' \in \mathscr{N}(T) \cap \mathscr{N}(T') \setminus \mathscr{N}_{h,\mathrm{D}}} (\nabla(u_{x',\mathrm{D}} - u_h), \nabla w_{T'})_{T'} \\ &\leqslant c_{26} \| R_{T'}(u_h) \|_{0,T'} \sum_{x' \in \mathscr{N}(T) \cap \mathscr{N}(T') \setminus \mathscr{N}_{h,\mathrm{D}}} h_{T'}^{-1} \eta_{x',\mathrm{D}}\end{aligned} \tag{4.23}$$

and

$$\begin{aligned}c_2^2 \| R_E(u_h) \|_{0,E}^2 &\leqslant (R_E(u_h), w_E)_E \\ &= \frac{1}{n'_x} \sum_{\substack{x' \in \mathscr{N}(T) \setminus \mathscr{N}_{h,\mathrm{D}} \\ x' \in E}} \Big\{ (\nabla(u_{x',D} - u_h), \nabla w_E)_{\omega_E} - \sum_{T'' \subset \omega_E} (R_{T''}(u_h), w_E)_{T''} \Big\} \\ &\leqslant c_{27} \| R_E(u_h) \|_{0,E} \sum_{\substack{x' \in \mathscr{N}(T) \setminus \mathscr{N}_{h,\mathrm{D}} \\ x' \in E}} \Big\{ h_E^{-1/2} \eta_{x',\mathrm{D}} + \sum_{T'' \subset \omega_E} h_E^{1/2} \| R_{T''}(u_h) \|_{0,T''} \Big\},\end{aligned} \tag{4.24}$$

where $n_x \in \{1, 2, 3\}$ and $n'_x \in \{1, 2\}$ are the numbers of nodes in $\mathcal{N}_{h,\Omega} \cup \mathcal{N}_{h,\mathrm{N}}$ which are shared by T and T' and by T and E, respectively. Estimates (4.23) and (4.24) immediately imply inequality (4.21). $\square$

The constants in Propositions 4.2–4.4 mainly depend on the shape regularity of the triangulation $\mathcal{T}_h$. When using an adaptive mesh generation technique as described in the Introduction, the latter essentially depends on the shape regularity of the coarsest mesh. Hence, a proper choice of the coarsest mesh may strongly influence the quality of the error estimators. A more detailed analysis of this aspect can be found in [4,13].

5. Adaptive mesh-refinement techniques

In this section we give a short overview on different mesh-refinement techniques. For a more detailed presentation and for comments on the required data structures, see [25] and the literature cited there. In what follows we will always assume that on a given mesh $\mathcal{T}_h$ we have computed local estimates η_T, $T \in \mathcal{T}_h$, of the true error of the finite-element discretization.

One possibility to obtain an optimal mesh is to minimize $\Sigma_{T \in \mathcal{T}_h} \eta_T^2$ under the constraint that the number of unknowns does not exceed a user-prescribed number (cf. [14]). This approach is rather costly.

Another possibility is to use some kind of local extrapolation to predict where further refinement may be advantageous. More precisely, assume that we have already computed η_T and $\eta_{T'}$, where T' is obtained by some refinement of T, and that we want to decide whether a further refinement of T' may be desirable. Then it is often quite reasonable to assume that the errors locally behave like ch_T^γ with unknown constants c and γ. One may use η_T and $\eta_{T'}$ to estimate c and γ. These estimates then give a prediction of the error on a refinement of T'.

Finally, one can heuristically argue that a mesh is optimal when the error is equidistributed [5,17]. This leads to the strategy: refine all T with $\eta_T \geqslant \gamma \max_{T' \in \mathcal{T}_h} \eta_{T'}$. Here, $0 < \gamma < 1$ is a given threshold, typically $\gamma = 0.5$. This strategy is very cheap and often yields satisfactory results. It is used in the numerical examples below.

Having decided which elements should be refined, one has to choose how to perform the actual refinement. This depends on the element geometry. For quadrilaterals it is most useful to refine them by connecting the mid-points of their edges. Triangles either may be cut into four new ones by connecting the mid-points of their edges or may be bisected by connecting the mid-point of one edge to the vertex opposite to it. The first possibility obviously produces similar triangles, whereas the second one may lead to increasingly acute triangles. Essentially two strategies have been developed to avoid this undesirable effect. In the *longest-edge bisection*, triangles may only be bisected by dividing their longest edge (cf. [18,19]). In the *marked-edge bisection*, triangles may only be cut along a marked edge. Initially one marks exactly one edge of each triangle in the coarsest mesh. When bisecting a triangle, its unmarked edges become the marked edges of the two new triangles (cf. [20]). For the refinement of tetrahedra, see [10]. For the comparison of different refinement strategies, see [16].

All these strategies must be complemented by rules how to cope with hanging nodes, i.e., points where condition (1) of Section 2 is violated. The simplest and most efficient way to do

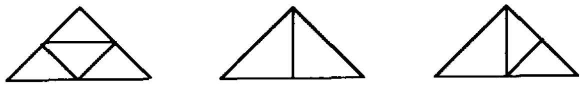

Fig. 3. Red, green and blue refinement of a triangle.

this for quadrilateral meshes is to treat the hanging nodes as spurious degrees of freedom, i.e., to fix the value of the finite-element functions in these points to be a suitable interpolation of their values corresponding to neighbouring regular nodes. For triangular meshes it is best to introduce auxiliary bisected triangles. Different strategies to avoid too acute auxiliary triangles are described in [25]. In the numerical examples below we use the following strategy.

When passing to the next triangulation, we call a triangle

(1) *red*, if it is cut into four new ones by joining the mid-points of its edges;

(2) *green*, if it is cut into two new triangles by joining the mid-point of the longest edge to the vertex opposite to this edge; and

(3) *blue*, if it is cut into three new triangles by joining the mid-point of its longest edge to the vertex opposite to this edge and to the mid-point of one of the remaining edges (see Fig. 3).

Then hanging nodes are avoided using the following rules.

(1) A triangle having three hanging nodes is *red*.

(2) A triangle having two hanging nodes is *blue*, if one of them lies on the longest edge of the triangle; otherwise it is *red*.

(3) A triangle having one hanging node is *green*, if the hanging nodes lies on its longest edge; otherwise it is *blue*.

Note, that rules (2) and (3) may introduce new hanging nodes. However, one can prove that the refinement process according to the above rules is finite. Moreover, rules (2) and (3) guarantee that condition (2) of Section 2 is satisfied.

6. Numerical examples

We consider two numerical examples: problem (2.1) in a circular domain $\Omega = \{(r, \phi): 0 \leqslant r < 1, 0 \leqslant \phi \leqslant \alpha\}$ with $\alpha = 1.5\ \pi$ for the first example and $\alpha = 2\pi$ for the second one and

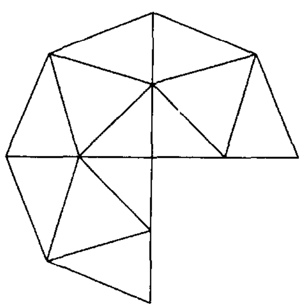

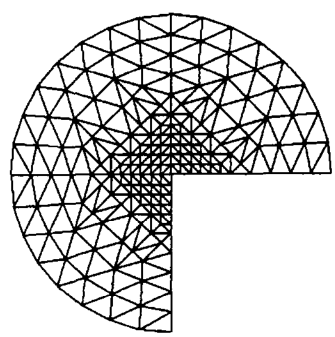

Fig. 4. Example 1, initial triangulation.

Fig. 5. Example 1, 4 refinement steps, 318 triangles, 183 nodes.

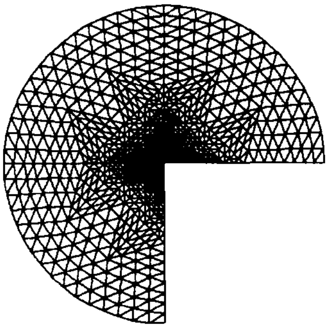

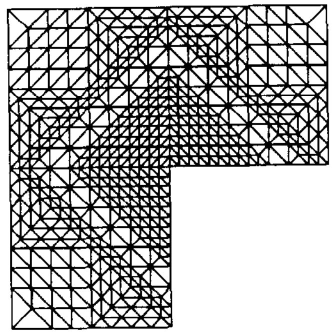

Fig. 6. Example 1, 7 refinement steps, 2298 triangles, 1209 nodes.

Fig. 7. Zoom of $[-\frac{1}{8}, \frac{1}{8}]\times[-\frac{1}{8}, \frac{1}{8}]$ in Fig. 6.

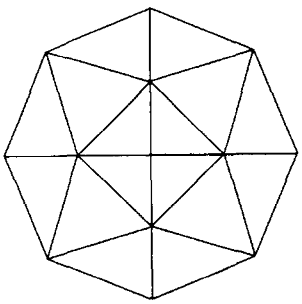

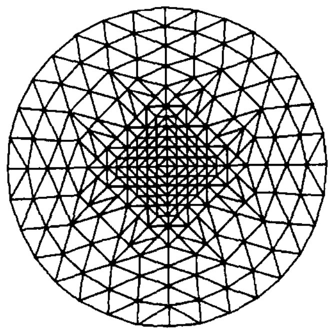

Fig. 8. Example 2, initial triangulation.

Fig. 9. Example 2, 4 refinement steps, 424 triangles, 240 nodes.

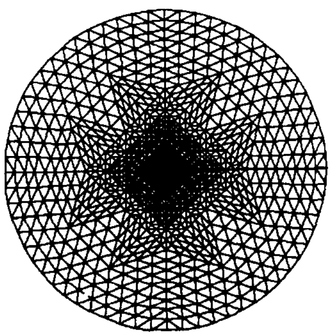

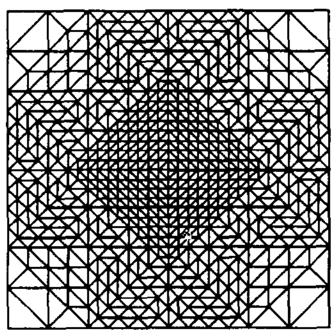

Fig. 10. Example 2, 7 refinement steps, 2832 triangles, 1482 nodes.

Fig. 11. Zoom of $[-\frac{1}{8}, \frac{1}{8}]\times[-\frac{1}{8}, \frac{1}{8}]$ in Fig. 10.

Table 1
Comparison of uniform and adaptive refinement

Example	Refinement	L	NT	NN	ϵ_u	q	Tt	Ts
1	Uniform	5	3072	1375	0.0175		10	107
	$\eta_{T,R}$	7	2298	988	0.0155	0.80	14	105
	$\eta_{T,\mathrm{N}}$	7	3108	1342	0.0106	0.95	51	190
	$\eta_{x,\mathrm{D}}$	7	2738	1213	0.0136	1.05	76	148
2	Uniform	5	4096	1371	0.0412		13	142
	$\eta_{T,R}$	7	2832	1240	0.0210	0.75	17	110
	$\eta_{T,\mathrm{N}}$	7	2678	1162	0.0217	0.90	42	98
	$\eta_{x,\mathrm{D}}$	7	2792	1220	0.0215	0.95	65	105

$f=0$ and $\Gamma_{\mathrm{D}}=\Gamma$ for both examples. For both examples, the exact solution is given in polar coordinates by

$$u=r^{\pi/\alpha}\sin\left(\frac{\pi}{\alpha}\phi\right).$$

The discretization uses continuous, piecewise linear finite elements, i.e., $k=1$. The error estimator is $\eta_{T,R}$. A triangle is refined if its estimated error is at least half of the estimated maximal error.

Figs. 4–11 show for all examples the initial triangulations together with two refined triangulations and zooms of the refinement near the critical regions. When using the estimator $\eta_{T,\mathrm{N}}$ or $\eta_{x,\mathrm{D}}$, the results are very similar.

Table 1 gives a comparison of uniform and adaptive refinement strategies for examples 1 and 2. Here L, NT, NN, ϵ_u, q, Tt and Ts are the number of refinement steps, the number of triangles, the number of unknowns, the relative error in the H^1-norm, the ratio of the predicted value of $\| u-u_h \|_{1,\Omega}$ to the true one, the time in seconds needed for mesh-generation, and the time in seconds required for the solution of the discrete problems. All computations were done on a MacIntosh IIx. Note that the solution algorithm could be accelerated, since it does superfluous work when only a few unknowns are added during the refinement process.

Table 1 shows that $\eta_{T,\mathrm{N}}$ and $\eta_{x,\mathrm{D}}$ give slightly better information about the numerical value of the error than $\eta_{T,R}$. Figs. 4–11, however, show that the latter efficiently detects the regions, where the mesh must be refined.

References

[1] S. Adjerid and J.E. Flaherty, A local refinement finite element method for two-dimensional parabolic systems, *SIAM J. Sci. Statist. Comput.* **9** (1988) 792–811.

[2] D.C. Arney and J.E. Flaherty, An adaptive local mesh refinement method for time-dependent partial differential equations, *Appl. Numer. Math.* **5** (4) (1989) 257–274.

[3] D.C. Arney and J.E. Flaherty, An adaptive mesh-moving and local refinement method for time dependent partial differential equations, *ACM Trans. Math. Software* **16** (1990) 48–71.

[4] I. Babuška, R. Duran and R. Rodriguez, Analysis of the efficiency of an a posteriori error estimator for linear triangular elements, *SIAM J. Numer. Anal.* **29** (4) (1992) 947–964.

[5] I. Babuška and W.C. Rheinboldt, Error estimates for adaptive finite element computations, *SIAM J. Numer. Anal.* **15** (1978) 736–754.
[6] I. Babuška and W.C. Rheinboldt, A posteriori error estimates for the finite element method, *Internat. J. Numer. Methods Engrg.* **12** (1978) 1597–1615.
[7] R.E. Bank and A. Weiser, Some a posteriori error estimators for elliptic partial differential equations, *Math. Comp.* **44** (1985) 283–301.
[8] R.E. Bank and B.D. Welfert, A posteriori error estimates for the Stokes equations: A comparison, *Comput. Methods Appl. Mech. Engrg.* **82** (1–3) (1990) 323–340.
[9] R.E. Bank and B.D. Welfert, A posteriori error estimates for the Stokes problem, Preprint, Univ. California, San Diego, CA, 1990.
[10] E. Bänsch, An adaptive finite-element strategy for the three-dimensional time-dependent Navier–Stokes equations, *J. Comput. Appl. Math.* **36** (1) (1991) 3–28.
[11] M. Bieterman and I. Babuška, The finite element method for parabolic equations. I A posteriori error estimation, *Numer. Math.* **40** (1982) 339–371.
[12] M. Bieterman and I. Babuška, The finite element method for parabolic equations. II A posteriori error estimation and adaptive approach, *Numer. Math.* **40** (1982) 373–406.
[13] R. Duran, M.A. Muschietti and R. Rodriguez, On the asymptotic exactness of error estimators for linear triangular elements, *Numer. Math.* **59** (1991) 107–127.
[14] H. Jarausch, On an adaptive grid refining technique for finite element approximations, *SIAM J. Sci. Statist. Comput.* **7** (1986) 1105–1120.
[15] C. Johnson, Yi-Yong Nic and V. Thomée, An a posteriori error estimate and adaptive timestep control for a backward Euler discretization of a parabolic problem, *SIAM J. Numer. Anal.* **27** (1990) 277–291.
[16] W.F. Mitchell, A comparison of adaptive refinement techniques for elliptic problems, *ACM Trans. Math. Software* **15** (4) (1989) 326–347.
[17] W.C. Rheinboldt, On a theory of mesh-refinement processes, *SIAM J. Numer. Anal.* **17** (1980) 766–778.
[18] M.-C. Rivara, Design and data structure of fully adaptive, multigrid, finite element software, *ACM Trans. Math. Software* **10** (1984) 242–264.
[19] M.C. Rivara, Algorithms for refining triangular grids suitable for adaptive and multigrid techniques, *Internat. J. Numer. Methods Engrg.* **20** (1984) 745–756.
[20] E.G. Sewell, Automatic generation of triangulations for piecewise polynomial approximations, Ph.D. Thesis, Purdue Univ., West Lafayette, IN, 1972.
[21] T. Strouboulis and J.T. Oden, A posteriori error estimation of finite element approximations in fluid mechanics, *Comput. Methods Appl. Mech. Engrg.* **78** (2) (1990) 201–242.
[22] R. Verfürth, A posteriori error estimators for the Stokes equations, *Numer. Math.* **55** (1989) 309–325.
[23] R. Verfürth, A posteriori error estimators and adaptive mesh-refinement for a mixed finite element discretization of the Navier–Stokes equations, in: W. Hackbusch and R. Rannacher, Eds., *Numerical Treatment of the Navier–Stokes Equations*, Notes Numer. Fluid Mech. **30** (Vieweg, Braunschweig, 1989) 145–152.
[24] R. Verfürth, A posteriori error estimators for the Stokes equations. II Nonconforming methods, *Numer. Math.* **60** (1989) 235–249.
[25] R. Verfürth, A posteriori error estimators and adaptive mesh-refinement techniques for the Navier–Stokes equations, in: M.D. Gunzburger and R.A. Nicolaides, Eds., *Incompressible CFD — Trends and Advances* (Cambridge Univ. Press, Cambridge, 1993) 1447–1475.